Polymer Degradation and Stability 193 (2021) 109715

Contents lists available at ScienceDirect

Polymer Degradation and Stability

journal homepage: www.elsevier.com/locate/polymdegradstab

A tetra-DOPO derivative as highly efficient flame retardant for epoxy resins

Wei Peng, Shi-bin Nie*, Yu-xuan Xu, Wei Yang

School of Safety Science and Engineering, Anhui University of Science and Technology, Huainan 232001, PR China

ARTICLE INFO

Article history:
Received 19 June 2021
Revised 19 August 2021
Accepted 28 August 2021
Available online 1 September 2021

Keywords:
Epoxy resins
Flame retardant
DOPO
Thermal property

ABSTRACT

In order to attain highly efficient flame retardant epoxy thermosets without deteriorating the thermomechanical performances, a 9,10-dihydro-9-oxa-10-phosphaphenanthrene 10-oxide (DOPO)-derived compound (tetra-DOPO) with different oxidation states of phosphorus and rich aromatic structures was successfully synthesized via addition and Atherton–Todd reactions. The molecular structure of tetra-DOPO was confirmed by the FTIR, ^{1}H- and ^{31}P-NMR spectra. The DMA measurement indicated that the addition of 5.0 wt% of Tetra-DOPO enhanced both the storage modulus and the glass transition temperature of the epoxy composite. The EP composite containing 5.0 wt% of Tetra-DOPO had an LOI of 30.0% and UL-94 V-0 grade, indicating the exceptional fire-retardant efficacy of tetra-DOPO. Additionally, in the cone calorimeter test, the PHRR, THR, and TSP values of EP/tetra-DOPO-5.0 were declined by 25.1%, 18.7%, and 13.9%, respectively, as compared to those of the EP. The reduced mean EHC value suggested the flame inhibition mechanism of tetra-DOPO in the vapor phase by emitting PO• radicals to quench the combustion chain reaction. The flame retardant mechanism of Tetra-DOPO was further clarified by detecting the pyrolytic gas species using TGA-FTIR as well as analyzing the microstructure of the char residues using SEM and Raman spectrometer. The main flame retardant mode of action of Tetra-DOPO was flame inhibition in the vapor phase, while it also played a relatively minor role in the condensed phase by forming an intact and compact char layer containing high graphitized structure.

1. Introduction

The utilization of flame retardant additives is the most cost-effective approach to obtain anti-flammable polymer materials. In recent years, halogen-free anti-flammable agents have been becoming the general trend and one of the hot research directions. Among a wide variety of halogen-free anti-flammable agents, phosphorus-based chemicals have been considered as one of the most promising flame retardants owing to their relatively high fire-retardant efficacy [1]. Over the past few decades, 9, 10-dihydro-9-oxa-10-phospaphenanthrene-10-oxide (DOPO) is one of the most famous phosphorus-based compounds for flame retardant epoxy resin [2–14]. DOPO is a mono-functional compound that reacts with the epoxy group via ring-opening reaction, leading to the reduced cross-linking density of the resulting cured epoxy products [15]. Thus, a series of DOPO derivatives have been synthesized to overcome the shortcomings of DOPO. Qian et al. synthesized a DOPO-derived flame retardant additive (HAP–DOPO) with cyclotriphosphazene as a core, and the epoxy thermosets containing 9.3 wt.% HAP–DOPO (1.2 wt.% phosphorus content) passed a UL-94 V-0 rating [12]. Zhang et al. reported a fire-retardant additive (DOPO-PEPA) for epoxy resins, and the epoxy thermosets with 9.1 wt.% DOPO-PEPA (1.4 wt.% phosphorus content) achieved an LOI value of 35% and a UL-94 V-0 rating [16]. Chen et al. synthesized a poly(piperazine phosphaphenanthrene) (DOPMPA) from DOPO and piperazine, and the addition of 13 wt.% DOPMPA endowed the resulting epoxy thermosets with an LOI value of 34% and a UL-94 V-0 rating [10]. Very recently, Wang et al. synthesized a phosphaphenanthrene/benzimidazolone-containing compound (POBDBI) as an anti-flammable agent for epoxy resin, and the incorporation of 13.4 wt.% POBDBI (1.0 wt.% phosphorus content) resulted in an LOI value of 36.5% and a UL-94 V-0 rating [17]. Battig et al. synthesized a rigid aromatic DOPO-derived hyperbranched flame retardant (PDTT) for flame retardant epoxy resins [18]. Although the epoxy with 10 wt. of PDTT cannot attain UL-94 V-0 grade, the total heat evolved and the peak heat release rate were decreased by 25% and 30%, respectively, owing to flame inhibition. Although these studies demonstrate the DOPO derivatives have imparted good flame retardant property to the epoxy thermosets, the relatively high addition amount of these DOPO derivatives usually cause the deteriorated thermomechanical prop-

* Corresponding author.
E-mail address: nieshibin88@163.com (S.-b. Nie).

https://doi.org/10.1016/j.polymdegradstab.2021.109715
0141-3910/

erties of the cured epoxy thermosets. Therefore, many researchers are still devoting themselves to the development of DOPO-derived flame retardants with high efficiency.

According to the previous studies, the integration of different oxidation states of phosphorus into one flame retardant molecule is conducive to flame retardant performance [16,19]. Generally, phosphorus with a lower oxidation state is more active in the vapor phase, whereas that with a higher oxidation state plays a predominant role in the condensed phase [1,20,21]. Since DOPO is a versatile platform for building the flame retardants, it can react with aldehydes or ketones through addition reaction to form a P-C bonding; as well, it can react with hydroxyl group through Atherton–Todd reaction to form a P-O bonding. Thus, it is interesting to integrate different oxidation states of phosphorus into one flame retardant molecule by combining addition and Atherton–Todd reactions. Furthermore, the bulky pendant DOPO units result in high structural stiffness, which is beneficial to the increment of glass transition temperature and mechanical property.

In this work, a tetra-DOPO derivative with different oxidation states of phosphorus and rich aromatic structure was successfully synthesized and implemented as a highly efficient anti-flammable agent for epoxy resins. The molecular structure of tetra-DOPO was confirmed by the Fourier transformed infrared (FTIR) spectroscopy, and ^{1}H- and ^{31}P-nuclear magnetic resonance (NMR) spectroscopy. The effect of tetra-DOPO on the thermomechanical and fire-retardant performances of the cured epoxy thermosets was studied, and the fire-retardant mode of action of tetra-DOPO was clarified eventually.

2. Experimental

2.1. Materials

Diglycidyl ether of bisphenol A (DGEBA, epoxy value: 0.44 mol/100 g) was purchased from Shanghai Macklin Biochemical Co., Ltd, China. 9, 10-dihydro-9-oxa-10-phospaphenanthrene-10-oxide (DOPO), 1, 4-phthalaldehyde (TDCA), and 4, 4'-diaminodiphenylmethane (DDM) were purchased from Shanghai Aladdin chemicals company, China. Toluene, dichloromethane, triethylamine, tetrachloromethane, and ethanol were purchased from Sinopharm Chemical Reagent Co., Ltd, China.

2.2. Synthesis of tetra-DOPO

TDCA-DOPO was synthesized according to the previous literature [5]. In a three necked round-bottom flask which equipped a nitrogen inlet, a thermometer and a condenser was filled with TDCA-DOPO (45.2 g, 0.08 mol) and DOPO (34.6 g, 0.16 mol), 200 mL dichloromethane, and triethylamine (17.2 g, 0.17 mol) in one portion. The mixture was cooled to below 5°C by ice bathing, and tetrachloromethane (26.15 g, 0.17 mol) was then dropped slowly in 60 min to ensure that the temperature did not exceed 20°C. After the completion of tetrachloromethane addition, the system was heated to ambient temperature and maintained stirring for another 17 h. Then, the precipitate was filtered, and the filtrate was evaporated using a rotary evaporator. The as-obtained crude product was recrystallized from 300 mL of ethanol, filtered and rinsed with water five times. The purified product was dried under vacuum at 80°C overnight to obtain a white powder. The synthetic route of the tetra-DOPO derivative is illustrated in Scheme 1.

2.3. Preparation of the cured epoxy thermosets

The tetra-DOPO powder was mixed with DGEBA epoxy resin at 100 °C under stirring for 1 h to yield a homogeneous mixture. Then, DDM was added to the above mixture at an equivalent molar ratio of N-H and epoxy groups. The mixture was stirred for another 10 min and then poured into the mold immediately. The curing process was 100 °C for 2 h, 150 °C for 2 h, and 180 °C for 1 h. The formulations of the cured epoxy thermosets containing 0, 2.5, and 5.0 wt% tetra-DOPO derivative are listed in Table 1. The epoxy thermoset was fabricated using the same way just without adding tetra-DOPO derivative.

2.4. Characterization

The molecular structure of the samples was determined by a Fourier transform infrared spectrometer (FTIR) (IRAffinity-1, Shimadzu) using a KBr disc method. The proton and phosphorus nuclear magnetic resonance (NMR) spectra were collected by an NMR spectrometer (AVANCE 400, Bruker) using deuterated dimethyl sulfoxide as solvent. The thermo-mechanical performance of the samples was measured by a dynamic mechanical analyzer (DMA) (Q850, TA Instruments). The samples with the dimensions of 50.0 mm × 10.0 mm × 3.0 mm was heated from 25 to 200 °C at a linear rate of 5 °C/min. Thermogravimetric analysis (TGA) was performed on a thermo-analyzer (TGA/SDTA851e, Mettler-Toledo) under both nitrogen and air conditions. The sample weighted about 5.0 mg was heated from ambient temperature to 700°C at a linear rate of 20°C/min. The limiting oxygen index (LOI) was determined on a TTech-GBT2406 oxygen index meter (TESTech Instrument Technologies Co., Ltd.) following the ASTM D2863−2017a specification. The sample size was 127 mm × 6.5 mm × 3.2 mm. The UL-94 vertical burning measurement was carried out by a CFZ-2-type apparatus (Nanjing Jiangning Analytical Instrument Co. Ltd.) following the ASTM D3801−2010 specification. The sample size was 127 mm × 12.7 mm × 3.2 mm. The flammability of the samples was measured using a cone calorimeter (Fire Testing Technology Ltd.) following the ISO 5660-1 specification. The heat flux used was 50 kW/m^2, and the sample size was 100 mm × 100 mm × 3 mm. The reported data were averaged from triple measurements. TGA-FTIR technique was employed to detect the pyrolytic gas species during the thermal degradation of the samples. A FTIR spectrometer (Nicolet 6700) was coupled with a thermo-analyzer (Q50, TA Instruments) through a transfer line. The sample was heated in the TGA from 25 to 800 °C at a linear rate of 20 °C/min under nitrogen condition. The pyrolytic gas products were sent to the gas cell of the FTIR spectrometer. The transfer line temperature was maintained at 230°C to avoid the condensation of pyrolytic gas species. The surface morphology of the chars was observed by a scanning electron microscopy (SEM) (Gemini 500, Carl Zeiss) at an accelerating voltage of 3 kV. The micro-structure of the chars was detected by a Laser confocal Raman spectrometer (inVia, Renishaw) using an excitation wavelength of 532 nm.

3. Results and discussion

The FTIR spectra of DOPO, TDCA-DOPO, and tetra-DOPO are depicted in Fig. 1. It can be seen that the characteristic bands of DOPO appear at 3062 cm^{-1} (Ph-H), 2434 cm^{-1} (P-H), 1594 cm^{-1} (C=C in the aromatic ring), 1236 cm^{-1} (P=O), 1119 and 950 cm^{-1} (Ph−O−P). In the FTIR spectrum of TDCA-DOPO, the absence of the characteristic band at around 2434 cm^{-1} (P-H in DOPO) [11] implies the completion of the addition reaction between DOPO and 1, 4-phthalaldehyde. In the FTIR spectrum of TDCA-DOPO, a new characteristic band appears at 3243 cm^{-1} corresponding to the hydroxyl group, and the signals of the cyclic DOPO structure are well preserved. For tetra-DOPO, the characteristic band at around 3243 cm^{-1} almost disappears, indicating the completion of the substitution reaction of TDCA-DOPO and DOPO.

The proton NMR spectra of DOPO, TDCA-DOPO, and tetra-DOPO are given in Fig. 2. It can be seen that the P-H signal at around

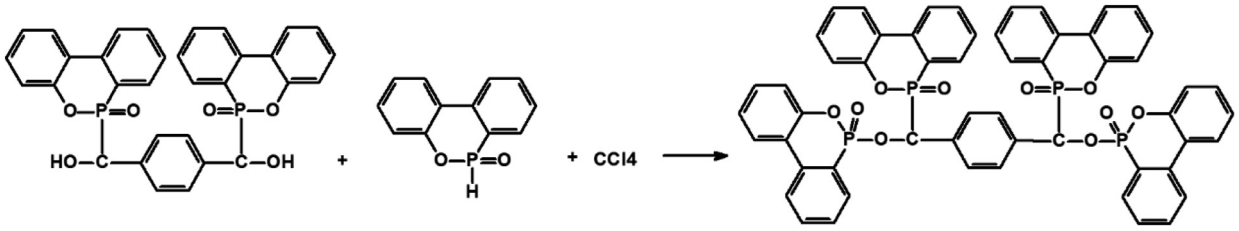

Scheme 1. The synthetic route of the tetra-DOPO derivative.

Table 1
The formulations of the cured epoxy thermosets.

Sample	DGEBA (g)	DDM (g)	Tetra-DOPO (g)	Theoretical P content (wt%)
EP	82.1	17.9	0	0
EP/Tetra-DOPO-2.5	80.0	17.5	2.5	0.31
EP/Tetra-DOPO-5.0	78.0	17.0	5.0	0.62

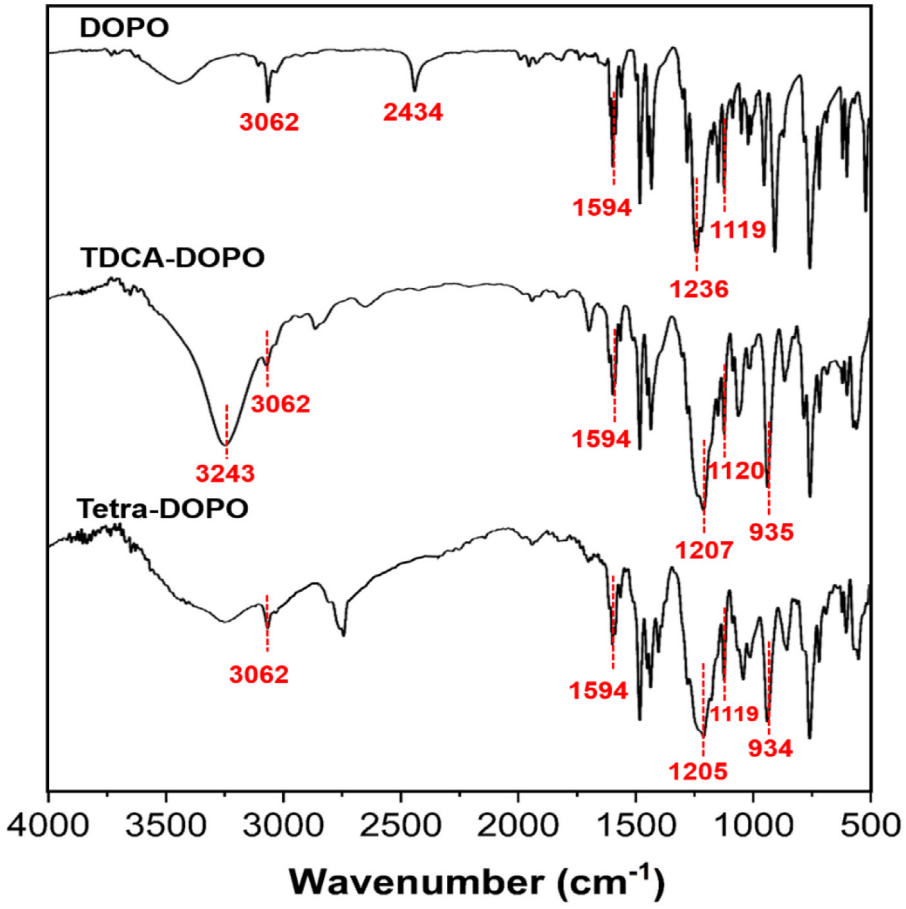

Fig. 1. FTIR spectra of DOPO, TDCA-DOPO, and tetra-DOPO.

8.90 ppm in the DOPO disappears in the proton NMR spectrum of TDCA-DOPO, implying the completion of the addition reaction between DOPO and 1, 4-phthalaldehyde. For TDCA-DOPO, a series of signals ranging from 7.10 to 8.30 ppm are allocated to the protons of aromatic rings, while the signals at 6.22–6.44 and 5.10–5.41 ppm are attributed to the hydroxyl and methyne protons, respectively [22], manifesting the successful synthesis of TDCA-DOPO. Compared with TDCA-DOPO, the signals of the hydroxyl protons disappear in the proton NMR spectrum of tetra-DOPO, implying the completion of the substitution reaction of TDCA-DOPO and DOPO. Besides, the chemical shift of the protons accords well with the expected structure of tetra-DOPO, confirming the successful synthesis of tetra-DOPO. The ^{31}P-NMR spectrum of TDCA-DOPO displays a single signal at 31.3 ppm (Fig. 3), corresponding to the DOPO unit linked by P-C bond. For tetra-DOPO, there are two distinctive signals at 31.3 and 21.8 ppm, corresponding to the linkage of DOPO units by P-C and P-O bonds, respectively. The FTIR and NMR results confirm the successful synthesis of tetra-DOPO.

The storage modulus and tanδ *versus* temperature curves are plotted in Fig. 4. The storage modulus at 30 °C of the EP is 1896 MPa, suggesting its high stiffness. After incorporating tetra-DOPO, the storage modulus at 30 °C of the EP/tetra-DOPO composites remains unchanged or even slightly increases, since the tetra-DOPO with rich aromatic structures has high rigidity. As the tempera-

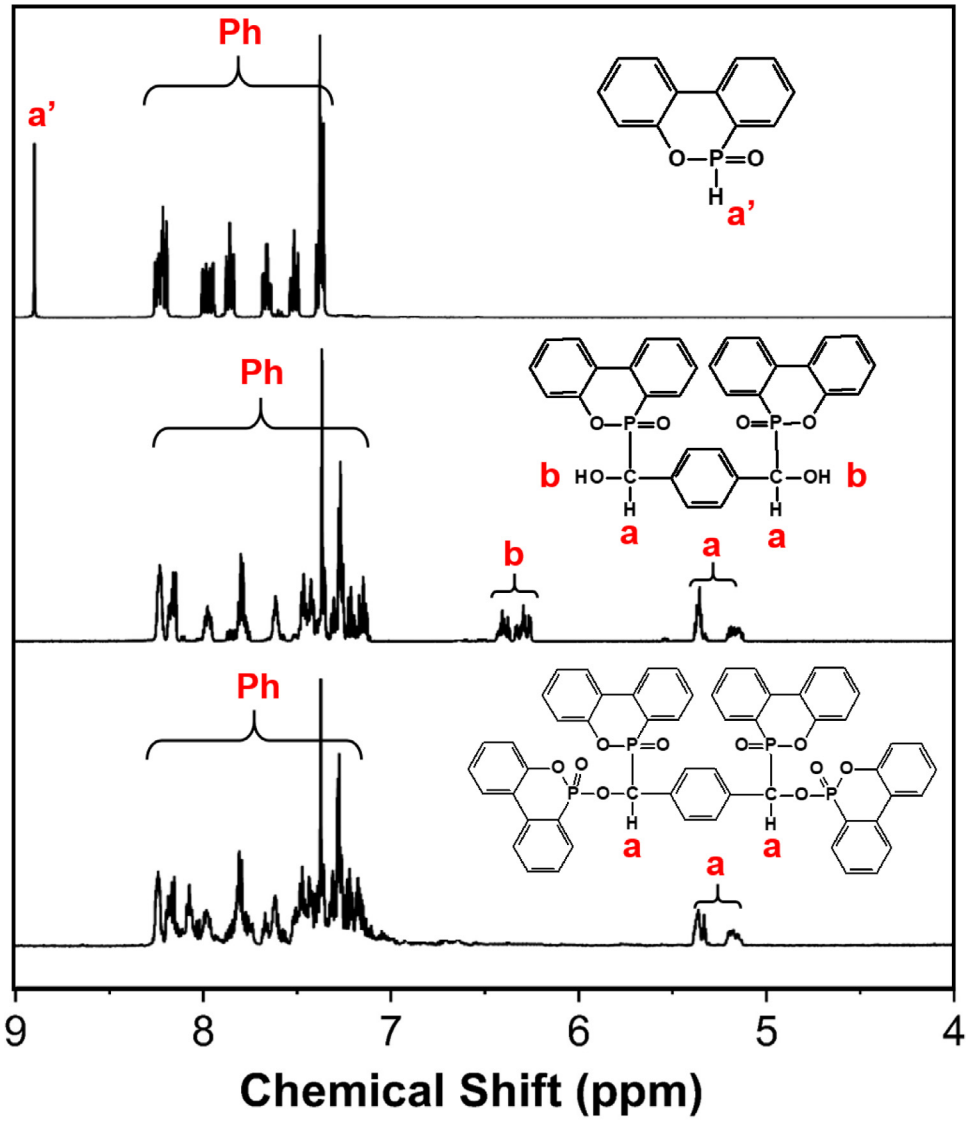

Fig. 2. ^{1}H-NMR spectra of DOPO, TDCA-DOPO, and tetra-DOPO.

ture increases, the storage modulus displays a decreasing trend, and there is a sharp reduction in the temperature range of 130-185 °C, corresponding to the glassy-rubbery state transition. The glass transition temperature (T_g) is obtained by the peak of tanδ *versus* temperature curves. The T_g of the EP is 151 °C, while that of the EP/tetra-DOPO-2.5 composite is increased to 165 °C because of the rigid structure of tetra-DOPO. Furthermore, the T_g of the EP/tetra-DOPO-5.0 composite is slightly reduced to 161 °C, which is ascribed to that the steric hindrance of bulky pendant DOPO unit decreases the cross-linking density at a higher dosage. However, the T_g of the EP/tetra-DOPO-5.0 composite is still 10 °C higher than that of the epoxy thermoset. The cross-linking density (υ_e) is computed by the following formula [23]:

$$\upsilon e = E'/3RT$$

where R is the gas constant (8.314 J/(mol•K)), E' is the storage modulus at 30 °C beyond T_g, and T is the Kelvin temperature. The υ_e of the EP, EP/tetra-DOPO-2.5, and EP/tetra-DOPO-5.0 is 1.32×10^3, 1.54×10^3, and 1.44×10^3 mol/m^3, respectively, which is consistent with the changing trend of the T_g values (Table 2).

The thermal decomposition behaviors of tetra-DOPO, epoxy resin and their tetra-DOPO composites under nitrogen and air are shown in Fig. 5. The specific data are depicted in Table 3. Under nitrogen, tetra-DOPO thermally decomposes in two steps with the maximum thermal decomposition temperature (T_{max}) of 221 and 367 °C. Tetra-DOPO also shows a low 5% weight loss temperature ($T_{-5\%}$) of 184 °C owing to the decomposition of thermally unstable phosphorus-based species. Eventually, tetra-DOPO yields only 8.3% residue, implying the poor charring capacity. All the epoxy samples have only one thermal degradation stage in the temperature range of 300 to 500 °C under nitrogen, which is attributable to the splitting of the three-dimensional macromolecular chains into some small molecular-weight compounds. Compared with EP, the $T_{-5\%}$ and the T_{max} of epoxy composites are decreased, implying that the existence of tetra-DOPO causes the early degradation of epoxy substrates. Besides, the addition of tetra-DOPO results in a very slight increment in the char yield at the high temperature, indicating the limited charring effect of tetra-DOPO in the condensed phase. Different from nitrogen, tetra-DOPO thermally decomposes in three steps with the T_{max} of 222, 376 and 605 °C. All the epoxy samples show two thermal degradation stages in air. The first stage in the temperature range of 300-470 °C is caused by the fracture of three-dimensional network of epoxy resin, while the second one in the temperature range of 500-650 °C corresponds to the further oxidation of the char. By contrast with EP, the $T_{-5\%}$ and T_{max} of the

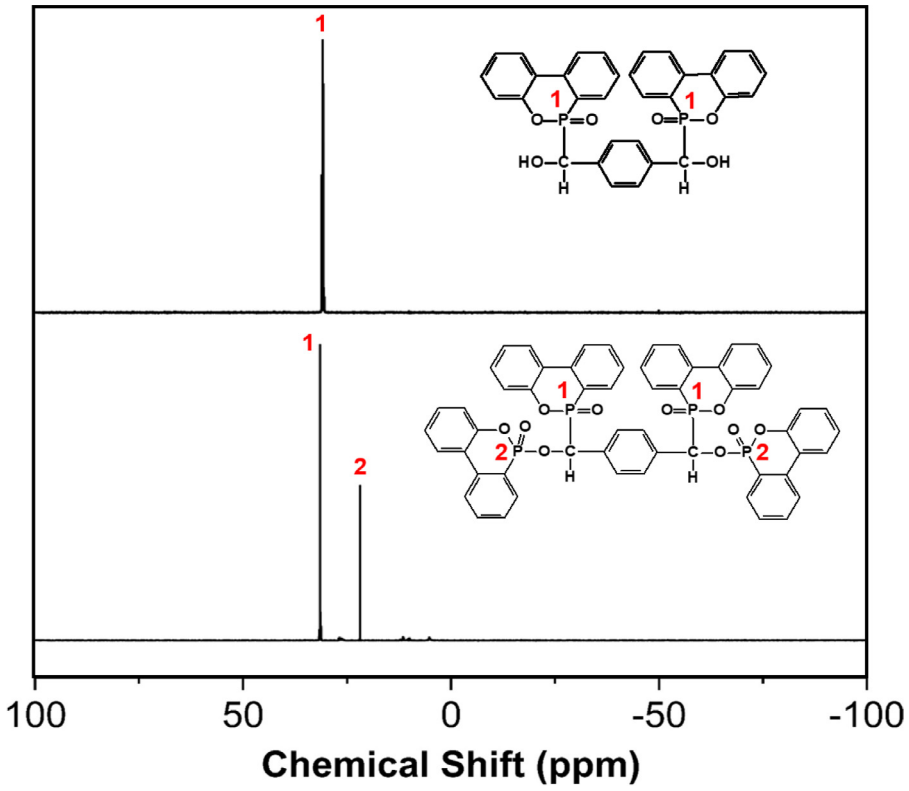

Fig. 3. ^{31}P-NMR spectra of TDCA-DOPO, and tetra-DOPO.

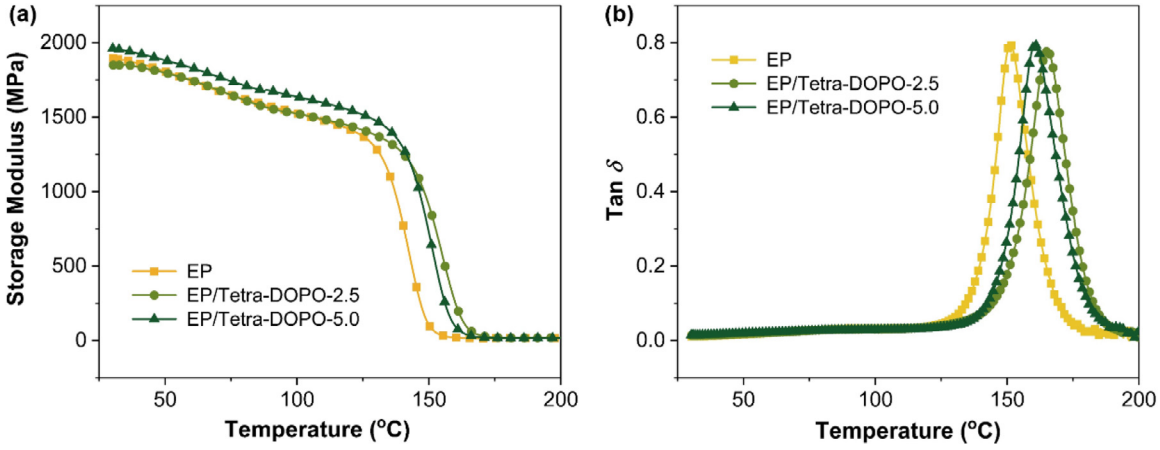

Fig. 4. (a) Storage modulus and (b) tanδ *versus* temperature curves of the cured epoxy thermosets.

Table 2
Thermo-mechanical parameters of EP and its composites.

Sample	T_g (°C)	E' at 30°C (MPa)	E' at T_g+30°C (MPa)	υ_e (mol/m^3)
EP	151	1896.2	15.0	1.32 × 10^3
EP/Tetra-DOPO-2.5	165	1850.3	18.0	1.54 × 10^3
EP/Tetra-DOPO-5.0	161	1962.1	16.7	1.44 × 10^3

Table 3
TGA and DTG data of the epoxy samples under the nitrogen and air atmospheres.

Samples	$T_{5\%}$ (°C ± 2)		T_{max} (°C ± 2)		Residues (% ± 1.0) at 700 °C	
	N_2	Air	N_2	Air	N_2	Air
Tetra-DOPO	184	175	221, 367	222, 376, 605	8.3	10.1
EP	369	367	381	378, 558	14.0	0.6
EP/Tetra-DOPO-2.5	347	345	362	360, 558	15.9	1.5
EP/Tetra-DOPO-5.0	335	336	350	349, 556	16.2	2.5

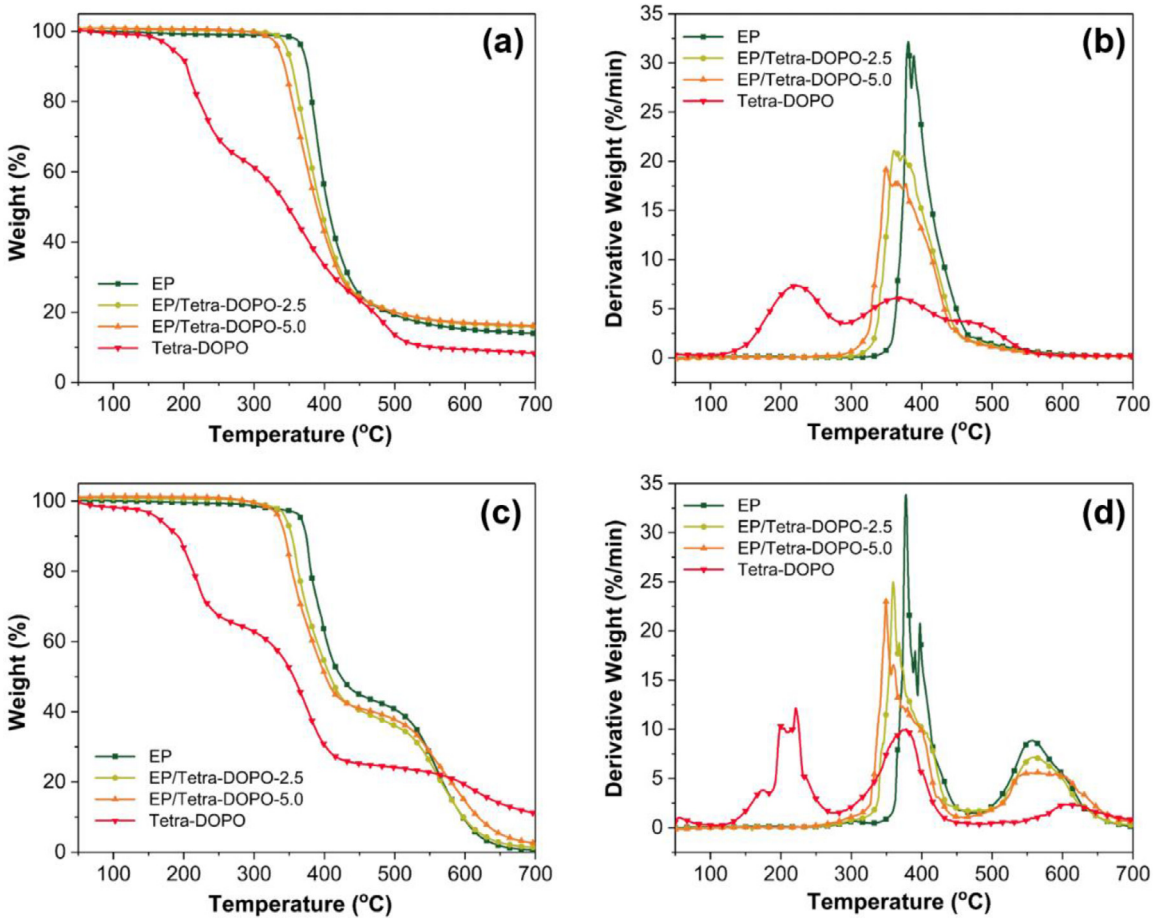

Fig. 5. (a, c) TGA and (b, d) DTG profiles of Tetra-DOPO and epoxy samples under nitrogen and air atmospheres.

Table 4
The results of the LOI and UL-94 vertical burning test of the cured epoxy thermosets.

Sample	LOI (%)	UL-94		
		t_1+t_2 *	Dripping	Rating
EP	23.5 ± 0.5	burning to clamp	Yes	Failed
EP/Tetra-DOPO-2.5	29.0 ± 0.5	14+5	No	V-1
EP/Tetra-DOPO-5.0	30.0 ± 0.5	4+3	No	V-0

Note: *t1 and t2 denote the burning time after the first and second ignition, respectively.

fire-retardant epoxy samples are declined, and the reason is similar to that under nitrogen. The yield of char residue at the high temperature under air atmosphere remains almost no change after the addition of tetra-DOPO, implying that the tetra-DOPO is not very effective in improving the carbonization of epoxy substrates.

The effect of the tetra-DOPO derivative on the flame-retardant behaviors of the cured thermosetting resins was studied by the means of LOI and UL-94 vertical burning test. The LOI and UL-94 vertical burning test results are summarized in Table 4. The EP thermoset shows an LOI value of 23.5% and no UL-94 grade, implying its poor flame resistance. The flame could not self-extinguish until the specimen was burnt out, with the melt dripping phenomenon. The cured epoxy thermoset containing 2.5 wt.% tetra-DOPO displays a relatively high LOI value of 29.0% and a UL-94 V-1 grade, and the melt dripping disappears. Further increasing the tetra-DOPO derivative content to 5.0 wt.% slightly improves the LOI of the cured epoxy thermoset to 30.0%, and the UL-94 V-0 grade is attained, implying the exceptional flame-retardant efficacy of tetra-DOPO.

The curves of heat release rate (HRR), total heat release (THR), total smoke production (TSP) and mass loss rate of EP and its tetra-DOPO composite with time are shown in Fig. 6. The specific parameters are depicted in Table 5. As shown in Fig. 6a and Table 5, the addition of tetra-DOPO decreases the t_{ig} of the epoxy composites compared to the epoxy, which is attributed to the earlier degradation of tetra-DOPO as also proved by the TGA results. Besides, the peak heat release rate of EP is 968 kW/m^2, and the PHRR of epoxy composite with 2.5wt% tetra DOPO is reduced to 805 kW/m^2, which is dropped by 16.8% as compared to that of EP. The PHRR value of EP /tetra-DOPO-5.0 composite is further reduced to 725 kW/m^2, which is dropped by 25.1% relative to that of EP. The trend of THR is similar to that of PHRR. As shown in Fig. 6b, the THR of EP is 157.5 MJ/m^2, and the THR of epoxy composite with 2.5wt% tetra-DOPO is reduced to 135.7 MJ/m^2, which is declined by 13.8% relative to that of EP. The THR value of EP/tetra-DOPO-5.0 composite is further decreased to 128.0 MJ/m^2, which is dropped by 18.7% relative to that of EP. The decrease of PHRR and THR of the composites indicates that tetra-DOPO can inhibit the heat release of epoxy matrix. In Fig. 6c, the TSP of pure EP is 33.2 m^2, while the TSP values of EP/tetra-DOPO-2.5 and EP/tetra-DOPO-5.0 composites are 31.4 and 28.6 m^2, respectively, which are declined by 5.4% and 13.9% as compared to that of pure EP. The reduction in TSR is less than the reduction in THR. Because cone calorimeter is a forced flaming condition, there is no smoke suppression, but the smoke yield increases. The increase in smoke yield may correspond with the flame inhibition. In Fig. 6d, the char yield of EP is

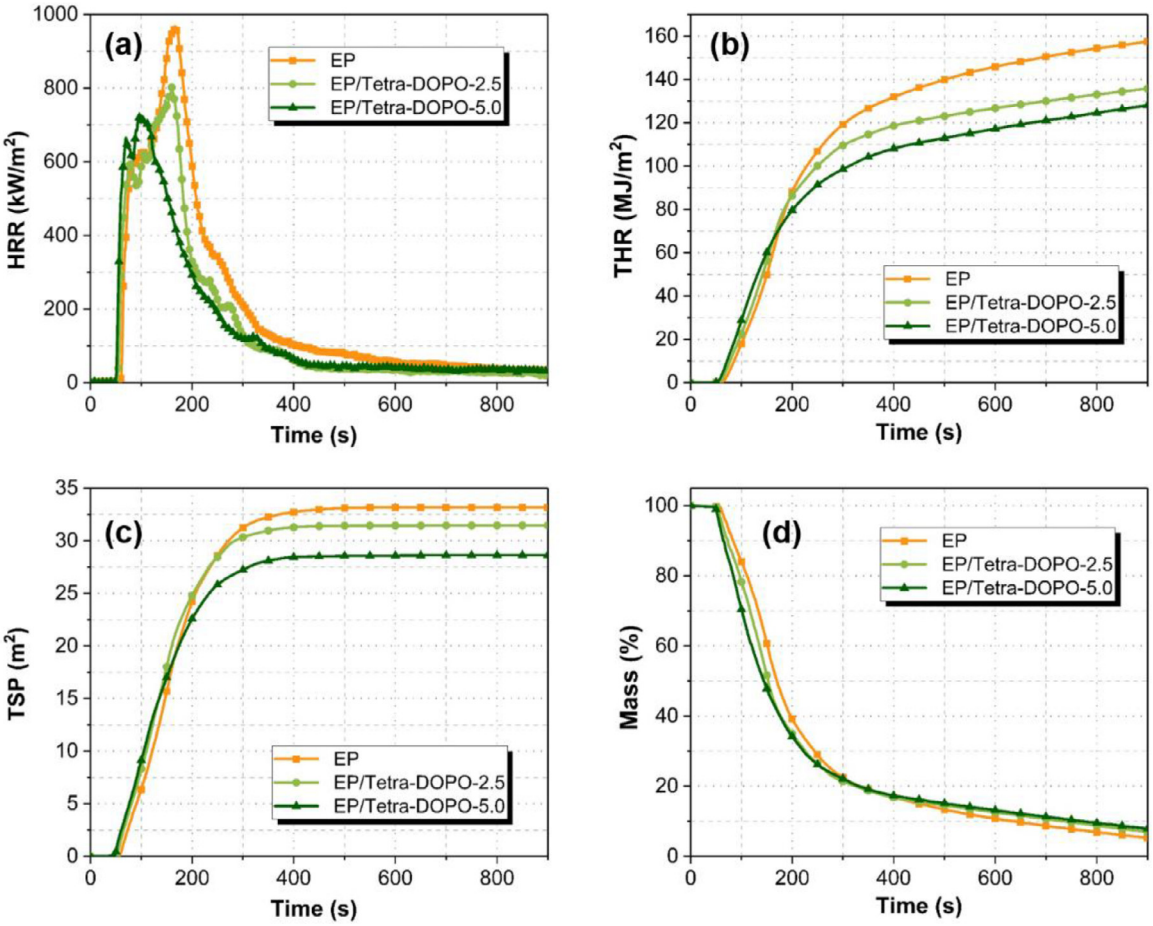

Fig. 6. (a) HRR, (b) THR, (c) TSP, and (d) mass loss versus time curves of the cured epoxy systems.

Table 5
Cone calorimeter data of the cured epoxy systems.

Samples	t_{ig}(s ± 2)	PHRR (kW/m² ± 40)	THR (MJ/m² ± 3.0)	TSP (m² ± 2.0)	Mean EHC (MJ/kg)	Residue (wt% ± 1.0)
EP	57	968	157.5	33.2	29.3	5.2
EP/Tetra-DOPO-2.5	50	805	135.7	31.4	26.2	6.9
EP/Tetra-DOPO-5.0	48	725	128.0	28.6	25.7	7.9

about 5.2%, whereas that of EP/tetra-DOPO-2.5 and EP/tetra-DOPO-5.0 is slightly grown to 6.9% and 7.9%, respectively. This slight difference is a difference in the thermo-oxidative stability of the fire residue. Mean effective heat of combustion (EHC) is an indicator of flame suppression in the vapor phase [24–26]. In Table 5, EP/tetra-DOPO-2.5 and EP/tetra-DOPO-5.0 display a lower mean EHC value than EP, suggesting that tetra-DOPO plays a flame suppression role in the vapor phase. This is because tetra-DOPO as a derivative of DOPO emits PO• radicals to quench the H• and OH• radicals [27], thus inhibiting the combustion chain reaction. Based on the analysis above, tetra-DOPO plays a predominant flame-retardant activity in the vapor phase as well as a relatively minor condensed phase mode of action.

TGA-FTIR was employed to detect the pyrolytic gas products of EP and EP/Tetra-DOPO-5.0 during the thermal degradation procedure. Fig. 7a and b provide the three-dimensional FTIR spectra of the vapor phase products of EP and EP/Tetra-DOPO-5.0. There are several intense absorbance peaks observed at the wavenumber range of 3700-3400, 3100-2800, 1800-1700, 1650-1450, and 1300-1100 cm^{-1}. The FTIR spectra of the vapor phase products of EP and EP/Tetra-DOPO-5.0 at the maximum degradation rate are given in Fig. 7c. Several characteristic absorbance peaks are identified at 3650 cm^{-1} (-OH stretching vibration in water), 2975 cm^{-1} (-CH_3 and/or -CH_2- stretching vibration), 1730 cm^{-1} (carbonyl stretching vibration), 1605 and 1510 cm^{-1} (C-C skeleton vibration), and 1175 cm^{-1} (C-O) [28]. After incorporating the Tetra-DOPO, the shape and position of the FTIR spectrum of the pyrolytic gas products of EP/Tetra-DOPO-5.0 are very similar to those of EP, implying that the majority of pyrolytic gas volatiles are the same as those of EP. However, the band of carbonyl stretching vibration at 1730 cm^{-1} of EP/Tetra-DOPO-5.0 has a lower intensity than that for EP, which results from the decreased carbonyl-containing products [18]. Thus, the TGA-FTIR results demonstrate that the presence of Tetra-DOPO changes the decomposition pathway of epoxy substrates, evidenced by the decreased carbonyl-moieties production.

Raman spectra were detected to explore the micro-structure of carbonaceous materials. As shown in Fig. 8, there are two intense peaks observed in the Raman spectra of the chars of EP, EP/Tetra-DOPO-2.5, and EP/Tetra-DOPO-5.0. The peak at around 1600 cm^{-1} is ascribed to the scattering of the crystalline carbon atoms in the graphited structure (named G-peak), while the other one at around 1360 cm^{-1} is caused by the scattering of the disordered carbon atoms in the amorphous zone (named D-peak) [29]. Generally, the graphited structure content of the chars is character-

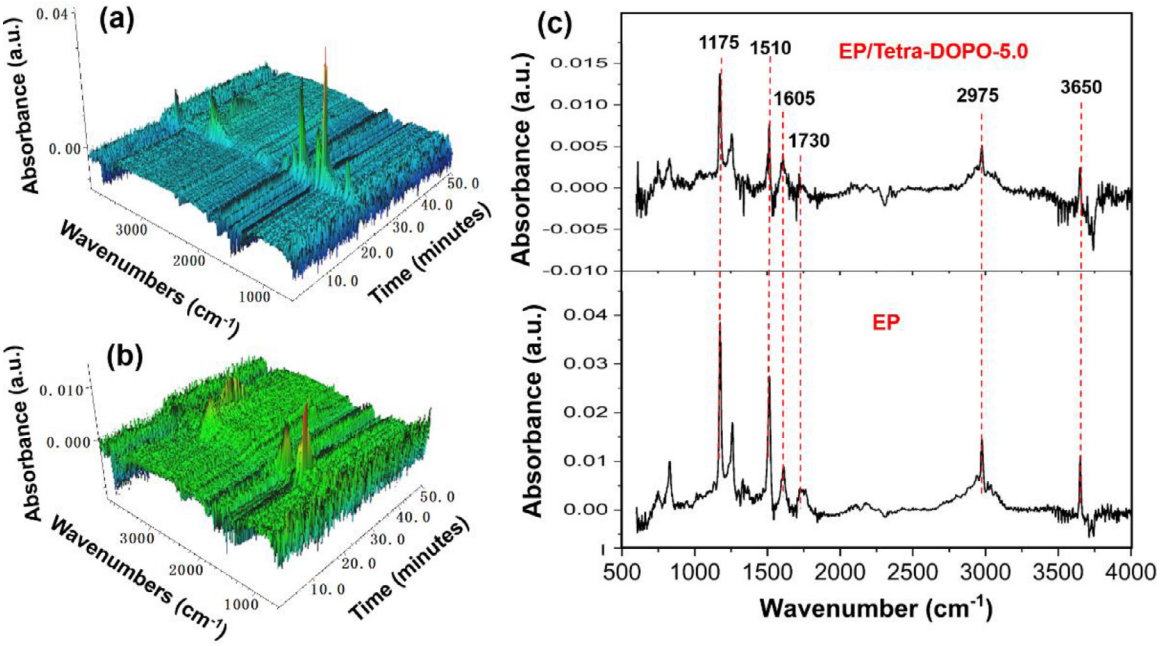

Fig. 7. Three-dimensional FTIR spectra of the pyrolytic gas products of (a) EP and (b) EP/Tetra-DOPO-5.0; (c) The FTIR spectra of the vapor phase products of EP and EP/Tetra-DOPO-5.0 at the maximum degradation rate.

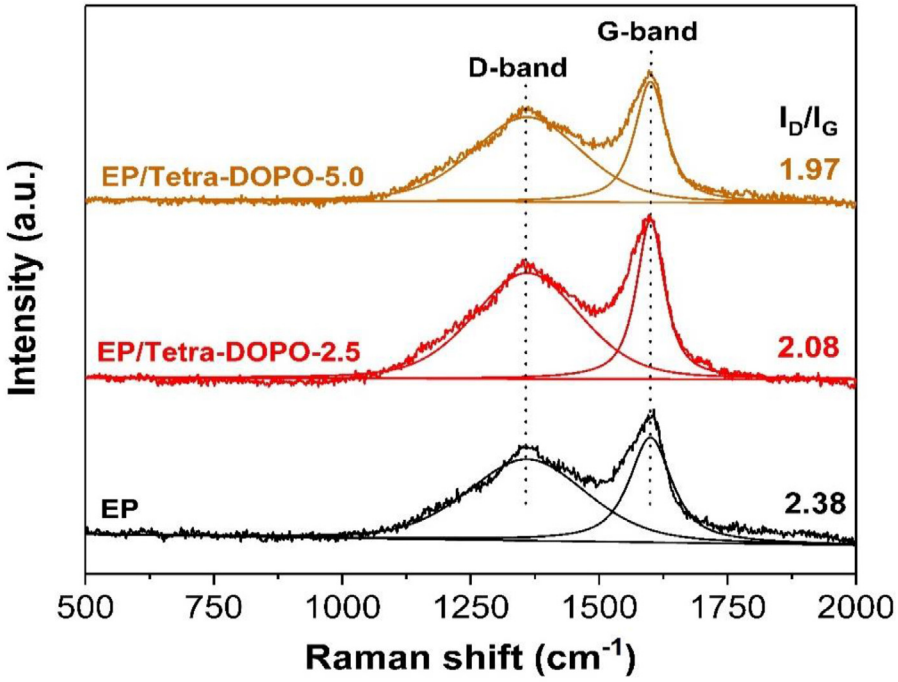

Fig. 8. Raman spectra of the chars of (a) EP, (b) EP/Tetra-DOPO-2.5, and (c) EP/Tetra-DOPO-5.0.

ized by the intensity between D-band and G-band (I_D/I_G) [30–32]. The I_D/I_G ratio of the char residues shows the following sequence: EP > EP/Tetra-DOPO-2.5 > EP/Tetra-DOPO-5.0. The higher I_D/I_G ratio implies the lower content of graphitized structure. The char residue of the EP/Tetra-DOPO-5.0 exhibits the lowest I_D/I_G ratio, meaning the highest graphited structure content. The higher graphited structure content in the residual chars is conducive to the enhanced resistance to heat.

Based on the discussion above, the flame retardant mechanism of Tetra-DOPO could be attributed to the synergism between phosphorus with different oxidation states in its structure. According to the previous report, phosphorus with lower oxidation state such as DOPO plays a dominant mode of action by releasing PO• radicals to quench the H• and OH• radicals in the vapor phase, while phosphorus with higher oxidation state serves as a char promoter in the condensed phase [1,21]. Tetra-DOPO contains phosphine and phosphonate simultaneously. Phosphine is highly active in the flame inhibition in the vapor phase (as evidenced by the reduced EHC), but phosphonate plays an inferior role in the charring capacity to phosphate (that is why the char yield is not high). Braun et al. reported that flame inhibition as a dominant mode of action plus minor carbonization was a quite effective route for fire retardancy

[6,33]. Thereby, Tetra-DOPO behaves high efficacy for flame retardant epoxy resins.

4. Conclusions

A tetra-DOPO derivative with different oxidation states of phosphorus and rich aromatic structures was synthesized successfully and implemented as an anti-flammable additive in epoxy resins. DMA measurement implied that the T_g of the EP/tetra-DOPO-5.0 composite was 10 °C higher than that of the EP thermoset. The TGA data indicated that the presence of tetra-DOPO derivative slightly changed the char yield. With 5.0 wt% addition of Tetra-DOPO, the resulting epoxy thermoset had an LOI of 30.0% and UL-94 V-0 grade, while the EP showed a much lower LOI of 23.5% and no UL-94 grade. In the cone calorimeter test, the PHRR, THR, and TSP values of the EP/tetra-DOPO-5.0 composite were 25.1%, 18.7%, and 13.9% lower than those of the EP, respectively. The high flame retardant efficacy of tetra-DOPO was attributed to the predominant vapor flame retardant mechanism by releasing PO• radicals to quench the combustion chain reactions as well as the minor condensed flame retardant mechanism by promoting epoxy matrix to form an intact and compact char layer containing high graphitized structure. This tetra-DOPO derivative provides a promising solution for highly efficient flame retardant epoxy thermosets without deteriorating the thermo-mechanical performances.

Declaration of Competing Interest

The authors declare that they have no known competing financial interests or personal relationships that could have appeared to influence the work reported in this paper.

CRediT authorship contribution statement

Wei Peng: Conceptualization, Methodology, Formal analysis, Writing – original draft. **Shi-bin Nie:** Funding acquisition, Project administration, Writing – review & editing. **Yu-xuan Xu:** Formal analysis. **Wei Yang:** Formal analysis.

Acknowledgement

The authors gratefully acknowledge Anhui Provincial Natural Science Foundation (1908085J20), University Synergy Innovation Program of Anhui Province (GXXT-2020-057, GXXT-2020-079) .

References

[1] M.M. Velencoso, A. Battig, J.C. Markwart, B. Schartel, F.R. Wurm, Molecular firefighting-how modern phosphorus chemistry can help solve the challenge of flame retardancy, Angew. Chem. Int. Edit. 57 (2018) 10450–10467.
[2] K.A. Salmeia, S. Gaan, An overview of some recent advances in DOPO-derivatives: chemistry and flame retardant applications, Polym. Degrad. Stabil. 113 (2015) 119–134.
[3] X. Wang, Y. Hu, L. Song, W. Xing, H. Lu, Thermal degradation mechanism of flame retarded epoxy resins with a DOPO-substituted organophosphorus oligomer by TG-FTIR and DP-MS, J. Anal. Appl. Pyrol. 92 (2011) 164–170.
[4] X. Wang, Y. Hu, L. Song, W. Xing, H. Lu, P. Lv, G. Jie, Flame retardancy and thermal degradation mechanism of epoxy resin composites based on a DOPO substituted organophosphorus oligomer, Polymer 51 (2010) 2435–2445.
[5] X. Wang, Y. Hu, L. Song, H. Yang, W. Xing, H. Lu, Synthesis and characterization of a DOPO-substitued organophosphorus oligomer and its application in flame retardant epoxy resins, Prog. Org. Coat. 71 (2011) 72–82.
[6] B. Perret, B. Schartel, K. Stöß, M. Ciesielski, J. Diederichs, M. Döring, J. Krämer, V. Altstädt, A new halogen-free flame retardant based on 9,10-dihydro-9-oxa-10-phosphaphenanthrene-10-oxide for epoxy resins and their carbon fiber composites for the automotive and aviation industries, Macromol. Mater. Eng. 296 (2011) 14–30.
[7] S.L. Jin, L.J. Qian, Y. Qiu, Y.J. Chen, F. Xin, High-efficiency flame retardant behavior of bi-DOPO compound with hydroxyl group on epoxy resin, Polym. Degrad. Stabil. 166 (2019) 344–352.
[8] P. Wang, F. Yang, L. Li, Z. Cai, Flame retardancy and mechanical properties of epoxy thermosets modified with a novel DOPO-based oligomer, Polym. Degrad. Stabil. 129 (2016) 156–167.
[9] P. Wang, L. Chen, H. Xiao, Flame retardant effect and mechanism of a novel DOPO based tetrazole derivative on epoxy resin, J. Anal. Appl. Pyrol. 139 (2019) 104–113.
[10] R. Chen, K. Hu, H. Tang, J. Wang, F. Zhu, H. Zhou, A novel flame retardant derived from DOPO and piperazine and its application in epoxy resin: flame retardance, thermal stability and pyrolysis behavior, Polym. Degrad. Stabil. 166 (2019) 334–343.
[11] P. Wang, Z. Cai, Highly efficient flame-retardant epoxy resin with a novel DOPO-based triazole compound: thermal stability, flame retardancy and mechanism, Polym. Degrad. Stabil. 137 (2017) 138–150.
[12] L.J. Qian, L.J. Ye, G.Z. Xu, J. Liu, J.Q. Guo, The non-halogen flame retardant epoxy resin based on a novel compound with phosphaphenanthrene and cyclotriphosphazene double functional groups, Polym. Degrad. Stabil. 96 (2011) 1118–1124.
[13] J.L. Wang, C. Ma, P.L. Wang, S.L. Qiu, W. Cai, Y. Hu, Ultra-low phosphorus loading to achieve the superior flame retardancy of epoxy resin, Polym. Degrad. Stabil. 149 (2018) 119–128.
[14] B. Schartel, U. Braun, A.I. Balabanovich, J. Artner, M. Ciesielski, M. Döring, R.M. Perez, J.K.W. Sandler, V. Altstädt, Pyrolysis and fire behaviour of epoxy systems containing a novel 9,10-dihydro-9-oxa-10-phosphaphenanthrene-10-oxide-(DOPO)-based diamino hardener, Eur. Polym. J. 44 (2008) 704–715.
[15] A. Schäfer, S. Seibold, O. Walter, M. Döring, Novel high Tg flame retardancy approach for epoxy resins, Polym. Degrad. Stabil. 93 (2008) 557–560.
[16] Y. Zhang, B. Yu, B. Wang, K.M. Liew, L. Song, C. Wang, Y. Hu, Highly effective P–P synergy of a novel DOPO-based flame retardant for epoxy resin, Ind. Eng. Chem. Res. 56 (2017) 1245–1255.
[17] H. Wang, S. Li, Z. Zhu, X. Yin, L. Wang, Y. Weng, X. Wang, A novel DOPO-based flame retardant containing benzimidazolone structure with high charring ability towards low flammability and smoke epoxy resins, Polym. Degrad. Stabil. 183 (2021) 109426.
[18] A. Battig, P. Muller, A. Bertin, B. Schartel, Hyperbranched rigid aromatic phosphorus-containing flame retardants for epoxy resins, Macromol. Mater. Eng. 306 (2021) 2000731.
[19] X.M. Zhao, H.V. Babu, J. Llorca, D.Y. Wang, Impact of halogen-free flame retardant with varied phosphorus chemical surrounding on the properties of diglycidyl ether of bisphenol-A type epoxy resin: synthesis, fire behaviour, flame-retardant mechanism and mechanical properties, RSC Adv. 6 (2016) 59226–59236.
[20] U. Braun, A.I. Balabanovich, B. Schartel, U. Knoll, J. Artner, M. Ciesielski, M. Doring, R. Perez, J.K.W. Sandler, V. Altstadt, T. Hoffmann, D. Pospiech, Influence of the oxidation state of phosphorus on the decomposition and fire behaviour of flame-retarded epoxy resin composites, Polymer 47 (2006) 8495–8508.
[21] B. Schartel, B. Perret, B. Dittrich, M. Ciesielski, J. Kramer, P. Muller, V. Altstadt, L. Zang, M. Doring, Flame retardancy of polymers: the role of specific reactions in the condensed phase, Macromol. Mater. Eng. 301 (2016) 9–35.
[22] Y.L. Liu, C.S. Wu, K.Y. Hsu, T.C. Chang, Flame-retardant epoxy resins from o-cresol novolac epoxy cured with a phosphorus-containing aralkyl novolac, J. Polym. Sci. Pol. Chem. 40 (2002) 2329–2339.
[23] S. Ma, X. Liu, Y. Jiang, L. Fan, J. Feng, J. Zhu, Synthesis and properties of phosphorus-containing bio-based epoxy resin from itaconic acid, Sci. China Chem. 57 (2014) 379–388.
[24] L. Zhong, K.X. Zhang, X. Wang, M.-J. Chen, F. Xin, Z.G. Liu, Synergistic effects and flame-retardant mechanism of aluminum diethyl phosphinate in combination with melamine polyphosphate and aluminum oxide in epoxy resin, J. Therm. Anal. Calorim. 134 (2018) 1637–1646.
[25] W. Xu, R. Chen, Y. Du, G. Wang, Design water-soluble phenolic/zeolitic imidazolate framework-67 flame retardant coating via layer-by-layer assembly technology: enhanced flame retardancy and smoke suppression of flexible polyurethane foam, Polym. Degrad. Stabil. 176 (2020) 109152.
[26] S. Liu, B. Yu, Y. Feng, Z. Yang, B. Yin, Synthesis of a multifunctional bisphosphate and its flame retardant application in epoxy resin, Polym. Degrad. Stabil. 165 (2019) 92–100.
[27] A. Schafer, S. Seibold, W. Lohstroh, O. Walter, M. Doring, Synthesis and properties of flame-retardant epoxy resins based on DOPO and one of its analog DPPO, J. Appl. Polym. Sci. 105 (2007) 685–696.
[28] Z. Zhang, C.J. Wang, G. Huang, H.R. Liu, S.L. Yang, A.F. Zhang, Thermal degradation behaviors and reaction mechanism of carbon fibre-epoxy composite from hydrogen tank by TG-FTIR, J. Hazard. Mater. 357 (2018) 73–80.
[29] X. Wang, S. Zhou, W. Xing, B. Yu, X. Feng, L. Song, Y. Hu, Self-assembly of Ni-Fe layered double hydroxide/graphene hybrids for reducing fire hazard in epoxy composites, J. Mater. Chem. A 1 (2013) 4383–4390.
[30] Z. Xu, W. Xing, Y. Hou, B. Zou, L. Han, W. Hu, Y. Hu, The combustion and pyrolysis process of flame-retardant polystyrene/cobalt-based metal organic frameworks (MOF) nanocomposite, Combust. Flame 226 (2021) 108–116.
[31] G. Tang, X. Liu, L. Zhou, P. Zhang, D. Deng, H. Jiang, Steel slag waste combined with melamine pyrophosphate as a flame retardant for rigid polyurethane foams, Adv. Powder Technol. 31 (2020) 279–286.
[32] G. Tang, X. Liu, Y. Yang, D. Chen, H. Zhang, L. Zhou, P. Zhang, H. Jiang, D. Deng, Phosphorus-containing silane modified steel slag waste to reduce fire hazards of rigid polyurethane foams, Adv. Powder Technol. 31 (2020) 1420–1430.
[33] B. Schartel, A.I. Balabanovich, U. Braun, U. Knoll, J. Artner, M. Ciesielski, M. Doring, R. Perez, J.K.W. Sandler, V. Altstadt, T. Hoffmann, D. Pospiech, Pyrolysis of epoxy resins and fire behavior of epoxy resin composites flame-retarded with 9,10-dihydro-9-oxa-10-phosphaphenanthrene-10-oxide additives, J. Appl. Polym. Sci. 104 (2007) 2260–2269.